WiSH: WiFi-based Real-Time Human Detection

Tianmeng Hang, Yue Zheng, *Student Member, IEEE,* Kun Qian, *Student Member, IEEE,* Chenshu Wu, *Member, IEEE,* Zheng Yang, *Member, IEEE,* Xiancun Zhou, *Member, IEEE,* Yunhao Liu, *Fellow, IEEE,* Guilin Chen, *Member, IEEE,*

Abstract—Sensorless sensing using wireless signals has been rapidly conceptualized and developed recently. Among numerous applications of WiFi-based sensing, human presence detection acts as a primary and fundamental function to boost applications in practice. Many complicated approaches have been proposed to achieve high detection accuracy, which, however, frequently omit various practical constraints like real-time capability, computation efficiency, sampling rates, deployment efforts, etc. A practical detection system that works in real world lacks. In this paper, we design and implement WiSH , a real-time system for contactless human detection that is applicable for whole-day usage. WiSH employs lightweight yet effective methods and thus enables detection under practical conditions even on resource-limited devices with very low signal sampling rates. We deploy WiSH on commodity desktops and customized tiny nodes in different everyday scenarios. The experimental results demonstrate superior performance of WiSH , achieving a detection accuracy of $> 98\%$ using a sampling rate of 20Hz with an average detection delay of merely 1.5s, which renders it a promising system for real-world deployment.

Index Terms—Human Detection; Channel State Information; Real-time System; Wireless Sensing; Off-the-shelf WiFi

1 Introduction

Wireless signals play a very important role in our daily lives. During old days they were usually used as a sole communication medium. Nowadays, they appear more frequently in sensing area [1]. Sensorless sensing has been quickly developed and enriched from both theoretical foundations and innovative applications. Received Signal Strength Indicator (RSSI) has been adopted in indoor localization systems. However, in complex situations, because of multipath fading and temporal dynamics it suffers from dramatic performance degradation . Channel State Information (CSI) is able to discriminate multipath characteristics and help analyze and capture human motions. A number of motivating applications have been enabled or improved, such as human detection [2], [3], human activity monitoring [4], gesture recognition and interaction [5], gait recognition [6], smoking detection [7], keystroke recognition [8], sleep monitoring [9], fall detection [10], respiration and heart rate monitoring [11], etc. While many researchers continue to foster more and more attractive applications with complicated design, we argue that building and validating simple and effective sensing systems that are applicable in practice is of equal importance and value to the community.

- *T.Hang, K.Qian, C.Wu, Z.Yang and Y.Liu are with the School of Software and TNLIST, Tsinghua University.*
  E-mail: hangtianmenglisa@gmail.com
- *Y.Zheng is with the Department of Electronic Engineering, and with the School of Software and TNLIST, Tsinghua University.*
  E-mail: zhengyue15@mails.tsinghua.edu.cn
- *X.Zhou is with the School of Information Engineering, West Anhui University.*
  E-mail: zhouxcun@mail.ustc.edu.cn
- *G.Chen is with the School of Computer and Information Engineering, Chuzhou University.*
  E-mail: glchen@chzu.edu.cn

Manuscript received October 15, 2017.

As dedicated or wearable sensors are too heavy for daily lives, many systems proposed to enable various human sensing applications without using them. But shortcomings are that they need strict requisites to be applicable in real environments. For example, dense links are deployed for accurate localization and tracking [12]. Sleep monitoring systems require users to be very close to the wireless links for sleep monitoring [9]. These systems may employ significant prior training for different locations for keystroke or activity recognition [4], [8], [13]. A truly practical wireless human sensing system that works in real world lacks. In this paper, we aim to design and implement a real-time system of contactless human detection, which works in practice for whole-day usage yet without resorting to impractical conditions like dense links, location-dependent prior trainings or interference-free environments, etc.

Human detection, a primary and fundamental function among plentiful applications, appears to be one of the most practically applicable killer applications, which is promising to be deployed in real world. Knowledge of human presence is a valuable primitive for security monitoring, smarthome monitoring, exhibition interaction, mall analytics, factory environment control, etc. Effective approaches have been proposed for human detection [2], [3], [14]. However, these methods still suffer from several limitations for real-time applications in practice. Typically, they usually require prior training, very high sample rate, and employ complex algorithms, rendering them infeasible for energy-efficient and real-time applications. In addition, most of existing systems are designed for arbitrary motion sensing that perceives any locomotion, instead of exact human detection that mainly targets at human presence events.

In this paper, we present WiSH , a lightweight system for real-time *Wi*reless *S*ensing of *H*uman detection. To boost applications in practice, WiSH employs an efficient detection algorithm that works with one single pair of transmitter and

receiver and very low sampling rates. Specifically, we extract simple but effective features from both time and frequency correlations of the received WiFi signals. On this basis, we design a robust event filter to deal with mis-alarms induced by instantaneous eruptions due to uncertain environmental dynamics. The key insight is that human presence events usually last for a certain duration. Thanks to its effectiveness and robustness, WiSH is widely applicable for whole-day deployment in different practical scenarios.

We implement WiSH on two types of devices: commodity desktops and laptops and customized embedded nodes, as shown in Fig. 1. The desktops are commodity mini PCs, while the customized nodes are tiny programmable routers that also support CSI measurement yet with much more limited computing resource. The tiny device is energy efficient, portable, easy to deploy, and most importantly, as cheap as about $10. A real-time system applicable on such nodes can be easily installed and is promising for practical everyday usage. WiSH executes the complete detection procedure as a standalone algorithm on end devices independently and announces detection events locally or outputs the detection results to a central server in real time, which then visualizes the detected events.

To evaluate the performance of WiSH , we deploy it in different scenarios such as lab offices, classrooms and home environments. We install a vision-based system to obtain the ground truths. We collect data for over 72 hours, which consists of over 300 movement events in total. The results demonstrate that WiSH achieves grateful detection performance even with very low sample rate of 20Hz on resource-limited devices. Specifically, WiSH yields an detection accuracy of >98%. The average detection delay is 1.5s while the durations of all detected events overlap with true events by 76.7%, which grows to 92.5% if the sampling rate increases to 90Hz.

In summary, our core contributions are as follow:

- We present WiSH , a real-time system for contactless human detection for whole-day usage. The design of WiSH fully accounts for various practical constraints including accuracy, detection delays, computation complexity, signal sampling rate, etc. and thus renders itself applicable for real-world deployment.
- We propose a lightweight method that harnesses both frequency and time correlations for motion sensing and employs a robust event filter for human detection, which enables effective human presence event detection even on resource-limited but easy-to-deploy devices with very low CSI sampling rates.
- We implement and deploy WiSH on commodity PCs as well as customized cheap and portable devices. The results demonstrate promising applicability of WiSH for practical daily monitoring.

The rest of paper is organized as follows. We describe the design goals in Section 2. The algorithms are presented in Section 3. System implementation and evaluation are provided in Section 4 and Section 5, respectively. We review the literature in Section 6 and conclude this paper in Section 7.

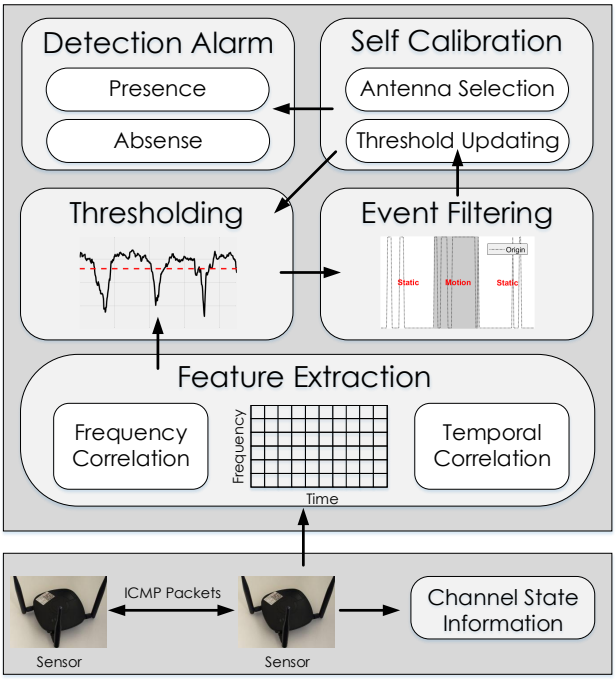

Figure 1. The framework of WiSH .

2 Design Space

2.1 Application Scenarios

Human detection is a long-standing and valuable problem that has attracted numerous efforts from both academic and industrial sides. Compared with previous detection manners like infra-red or vision-based approaches, WiFi-based systems have advantages in low costs, omni-directional coverage, through-wall capabilities, and privacy-preserving, etc. Hence WiFi-based sensorless sensing is useful in various applications.

Typically, wireless human detection can be used for intruder detection for home security, storehouse monitoring, hotel services. Take hotels as an example. The waiter should not disturb the customers if they are detected to be in the room via a privacy-friendly manner. Sleep monitoring can also benefit a lot from sensorless sensing. The experience would be largely enhanced if the light can be intelligently turned on/off with a system automatically sensing whether a person getting up in the night to urinate. Wireless sensing is also helpful to smarthome and smart building analytics. By analyzing the presence durations and patterns of a user at home, building architects are able to improve the indoor space design. As a primitive, all these applications demand a practical and easy-to-deploy system that is capable of whole-day detection of human presence in real time.

2.2 Design Goals

We expect WiSH to be a practical human detection system for whole-day monitoring. To achieve this goal, the system should meet the following properties.

- Accurate and robust. WiSH should accurately detect human presence events, yet reduce the false alarms to the minimum extents.

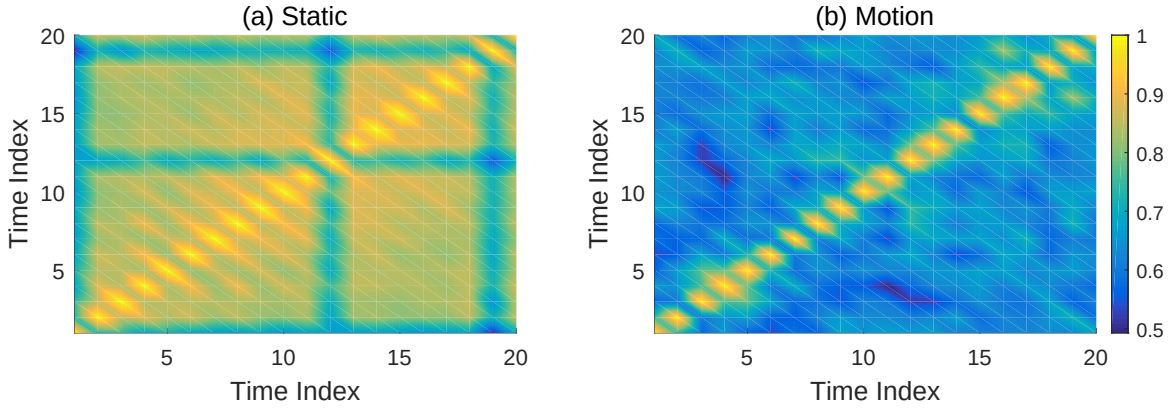

Figure 2. Distribution of temporal correlation of CSI in (a) static cases and (b) motion cases.

- Real-time. WiSH should detect and report human presence events in real-time. Delay-sensitive applications like intruder detection may require instantaneous results for emergence responses.
- Energy efficient. We envision the capability of human sensing to be integrated in general communication devices, or installed on battery-powered devices in the future. Thus the energy consumption, either by CSI sampling or computation, should be as low as possible.
- Low sampling rate. WiSH works on communication devices in a non-invasive way. To restrict the impacts on communication itself, a detection system should yield reasonable accuracy with very low sample rates.

Most existing systems achieve good performance, yet rely on pretty high sample rate (e.g., 100Hz to 1000kHz [2], [15]) and do not work in real time. In this paper, we design and implement WiSH , which is expected to be capable of real-time detection for whole-day applications. In contrast to mainly considering detection precision, WiSH targets at real-world applicability and fully accounts for various practical constraints including real-time capability, energy efficiency, sampling rate limitation, computation complexity, deployment efforts, etc.

3 Methods

3.1 System Flow

WiSH is a system that utilizes Channel State Information (CSI) to implement human detection. CSI depicts channel properties of a wireless link and is provided by off-the-shelf network interface cards (NIC) with slight driver modification. In static/dynamic environments, CSI will exhibit different characteristics. Thus CSI will be a favourable indicator of moving human with proper features extracted. As we aim to implement real-time human detection, latency, computational cost and energy cost should be also considered when designing features. How to propose a light-weight detection algorithm is the first challenge we need to undertake. Furthermore, due to the presence of noise and radio frequency interference, CSI might not be stable even if there is no moving targets. False alarms will arise if we cannot filter the exceptional events out. Therefore, the second challenge is to implement a robust event filter based on the observation that dynamic changes of the propagation environment induced by human usually lasts for a sufficiently long duration. Besides, we find that different antennas of the receiver might suffer different degrees of dynamics when a person is walking. And channel properties might vary even if the surroundings change a little. In order to promote the robustness and sensitiveness of the system, it is necessary to adopt suitable self-calibration mechanism.

Fig. 1 depicts the overall framework of WiSH . The system first retrieves CSI by exchanging ICMP packets between sensors. The obtained CSI is then fed into the upper layer for further processing. First, features of correlation in both time and frequency domain are calculated. Then, a threshold is applied to the features to preliminarily detect moving entities in the monitor area. The preliminary noisy detection result is further filtered based on the limitation of the minimum length of moving event. With trustworthy groundtruth obtained during specific time such as midnight when there are likely no moving entities in the monitor area, self calibration is performed by the system to select stable antennas as well as update the preliminary threshold. The system alarms once the output indicates the existence of moving entities.

3.2 Detection Algorithm

With CSI Tool [16] deployed on commodity WiFi devices, CSI can be collected in the following format:

$$H = [H(f_1), H(f_2), ..., H(f_k), ..., H(f_N)]^T, k \in [1, N] \quad (1)$$

where N denotes the total number of subcarriers in an OFDM symbol and f_k denotes the central frequency of the kth subcarrier. $H(f_k)$ is defined as

$$H(f_k) = |H(f_k)|e^{j\angle H(f_k)} \quad (2)$$

where $|H(f_k)|$ and $\angle H(f_k)$ denote the amplitude and phase respectively. Raw phase information usually behaves random due to noise, packet boundary detection uncertainty, central frequency offset and sampling frequency offset [17]. Thus we only utilize the amplitude of CSI to detect movement events.

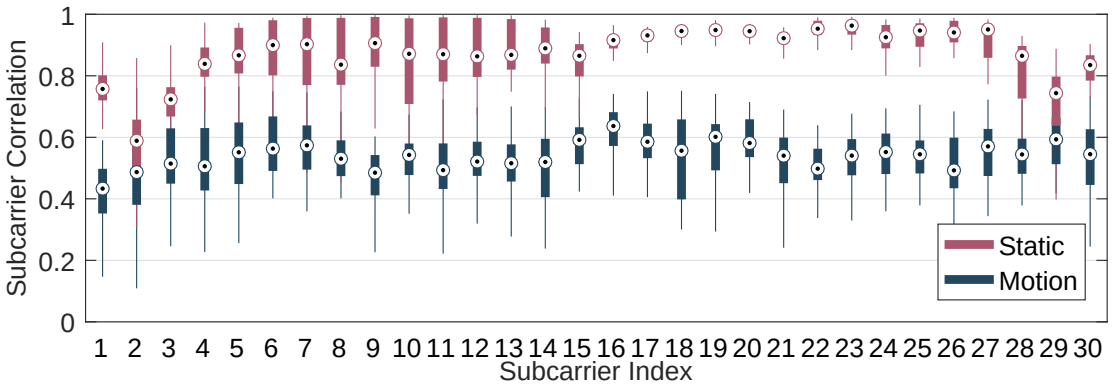

Figure 3. Distribution of frequency correlation of CSI.

To implement the human detection algorithm, we first collect continuous CSI measurements over a sliding window W. Suppose that the sliding window consists of T CSI measurements under a specific sampling rate, then a matrix M in time-frequency domain can be expressed as:

$$M = [H_1, H_2, ..., H_T] = [S_1^T, S_2^T, ..., S_F^T]^T; \quad (3)$$

where H_i denotes the CSI collected at the i-th sampling time in the sliding window, and S_j denotes the CSI sequence of the j-th subcarrier.

The core idea of motion detection is to quantize variations of CSI. However, simply calculating variances of CSI suffers from hardware issues such as power control. Instead, we use correlation of CSI in both time and frequency to indicate the existence of movement events. Specifically, in time domain, we calculate cross-correlation of each pair of CSI. Fig. 2 shows the average cross-correlation of different pairs of CSI in a sliding window. Intuitively, when the environment is static, all CSI in the sliding window are highly correlated, with cross correlation higher than 0.95. In contrast, when there exists entities moving in the environment, the cross correlation between different CSI significantly decreases to about 0.8.

In addition to time domain, we further study the correlating property of CSI in frequency domain. Specifically, the cross correlation of CSI sequences of different subcarriers is calculated. Fig. 3 plots the distribution of cross correlation in frequency domain in the presence and absence of moving entities. The dot on each subcarrier bar means median of cross correlation in frequency. Clearly, the existence of moving entities statistically decreases the cross correlation of most subcarriers. However, the variation of frequency correlation is not that stable in comparison with time correlation. To leverage cross correlation in both time and frequency domain, we select median values of both correlation data, and integrate both correlation as motion indicator (MI):

$$MI = \bar{c}_t e^{0.1\bar{c}_f} \quad (4)$$

where $\bar{c}_t$ is the median value of time correlation and $\bar{c}_f$ is the median value of frequency correlation. A coefficient of 0.1 and the exponential operator are used to accommodate the noisy fluctuation of frequency correlation and we use training data to find the most suitable coefficient. A threshold is applied for the motion indicator MI to preliminarily detect motion of entities in the monitor area. Note that movement events result in lower values of MI, and we regard such MIs as positive in this paper.

In particular, when we calculate cross correlation in frequency, we do not have to calculate all the cross correlation between every subcarrier, instead we randomly select some subcarriers from all subcarriers and only calculate their cross correlation. With this method operation time is largely shortened and overall performance is almostly similar. Detection algorithm is detailed in Algorithm 1.

Algorithm 1: Motion Indicator (MI) Calculation

Input: M: $F \times T$ CSI matrix
Output: MI: Motion indicator

/* Calculate correlation of CSI samples*/
for all $t_1, t_2 = 1 \dots T$ **do**
  $c_t(t_1, t_2) = \frac{H_{t_1}^T H_{t_2}}{\|H_{t_1}\| \|H_{t_2}\|}$
end for
$\bar{c}_t = \text{Median}(c_t(t_1, t_2))$

/* Calculate correlation of CSI subcarriers*/
Randomly pick a certain number of subcarriers from all subcarriers
for all $f_1, f_2 = 1 \dots F$ **do**
  $c_f(f_1, f_2) = \frac{S_{f_1} S_{f_2}^T}{\|S_{f_1}\| \|S_{f_2}\|}$
end for
$\bar{c}_f = \text{Median}(c_f(f_1, f_2))$

/* Calculate Motion Indicator */
$MI = \bar{c}_t e^{0.1\bar{c}_f}$

3.3 Robust Event Filter

WiFi operates in the free 2.4/5 GHz ISM band, which is exceedingly crowded especially in modern buildings. Apart from our own system, a great number of radio devices are also working and we can hardly find an interference-free channel. In order to resist interference, a WiFi receiver might adjust power to guarantee correct decoding. It might also change modulation and coding scheme (MCS) index

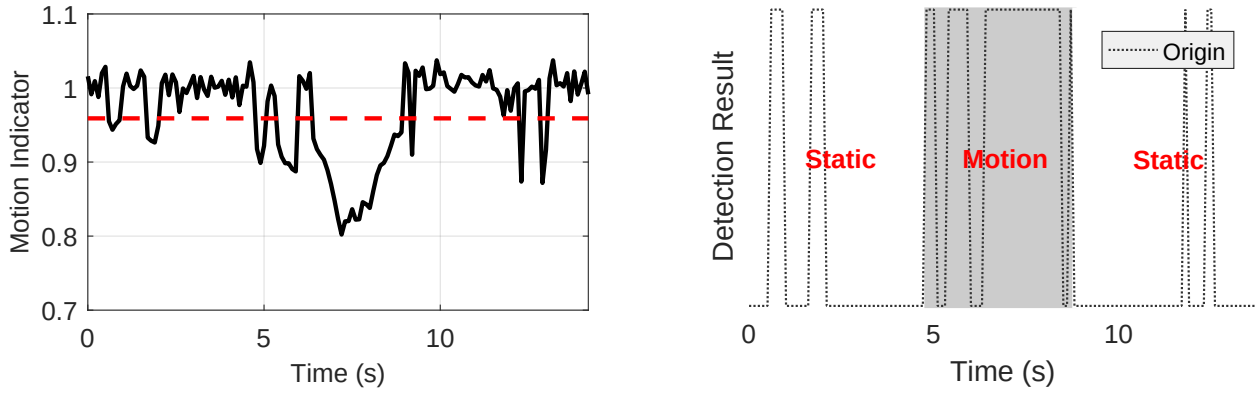

(a) Determine a movement event.

(b) Splice adjacent movement events

Figure 4. Examples of event filter.

Algorithm 2: Event Filter

Input:
MIS: $1 \times T$ Motion indicator sequence
ϵ: Threshold for motion indicator
d_1, d_2: Thresholds for event filter
Output: DS: $1 \times T$ Detection sequence

/* Detection with rough threshold */
for all $t = 1 \dots T$ **do**
  $DS_t = \{MIS_t < \epsilon\}$
end for

/* Filter false alarms of motion */
for Successive $DS_{t \dots t+L+1}$ **do**
  if $DS_t = 0$ and $DS_{t+L+1} = 0$ **then**
    if $DS_{t \dots t+L-1} = 1$ and $L < d_1$ **then**
      $DS_{t \dots t+L-1} = 0$
    end if
  end if
end for

/* Filter static false alarms */
for Successive $DS_{t \dots t+L+1}$ **do**
  if $DS_t = 1$ and $DS_{t+L+1} = 1$ **then**
    if $DS_{t+1 \dots t+L} = 0$ and $L < d_2$ **then**
      $DS_{t+1 \dots t+L} = 1$
    end if
  end if
end for

when the communication quality of the channel degrades. Both of above result in the observation that CSI amplitude suffers abrupt fluctuations occasionally. And false alarms will arise if there is a sufficient number of exceptional CSI measurements in the sliding window.

With the aim of decreasing false alarms, we propose a robust event filter based on the observation that human presence events usually last for a sufficiently long time. Eruptions induced by interference, in contrast, do not appear continuously. Now we formally illustrate how the event filter works. Suppose that for sliding widow W_i, the corresponding motion indicator MI_i is determined to be positive status. Then we observe following motion indicators continuously. Only when all the values in the sequence $MI_i, MI_{i+1}, ..., MI_{i+d_1-1}$ are lower than the threshold will the system alarm the presence of moving entities (see Fig. 4a). Besides, as we adopt a fixed threshold for motion indicators, human movements might be ignored if the corresponding MIs just fluctuate around the threshold. The phenomenon is not uncommon as the impacts that human movements exert on CSI might degrade at specific locations. Therefore, as long as the interval between two positive motion indicators MI_j and MI_k is less than d_2, we regard the sequence $MI_j, MI_{j+1}, ..., MI_k$ as positive (see Fig. 4b). The pseudo code is shown in Algorithm 2.

3.4 Self-calibration

For both detection algorithm and event filter, thresholds need to be determined preliminarily through training when the system is deployed. Besides, as the environment settings might vary and channel properties also change, the value of thresholds might need to be recalibrated over a few days. A heuristic approach is to exploit the data collected after midnight (e.g., 3:00∼4:00 am) for recalibration because there are hardly moving entities.

The performance of WiSH is also sensitive to antenna choice. As different antennas of the WiFi receiver corresponds to different propagation environment, CSI collected by each antenna is distinctive. And the dynamics of CSI induced by moving entities are at different degrees. Thus the sensitiveness of the antenna is crucial in detection accuracy. If the antenna is rather insensitive, tiny movements will be concealed. On the other hand, the performance will also degrade if the antenna is too sensitive. In such case, noise can be also regarded as movements and false alarms arise. Therefore, to discard the improper antenna is critical. WiSH can automatically achieve antenna selection via detection accuracy comparison when recalibrating the thresholds.

4 Implementation

To deploy WiSH , we use two tiny WiFi nodes (the appearance is shown in Fig. 5) which can work as the transmitter

Figure 5. Tiny sender node.

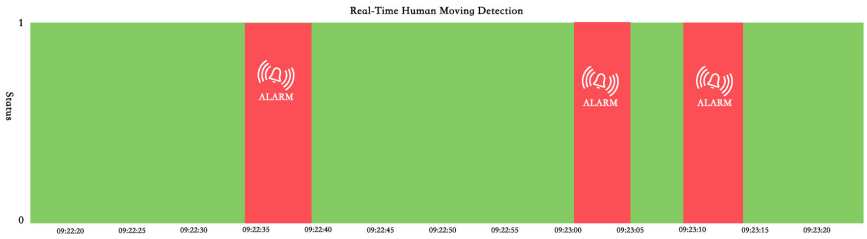

Figure 6. The real-time GUI website.

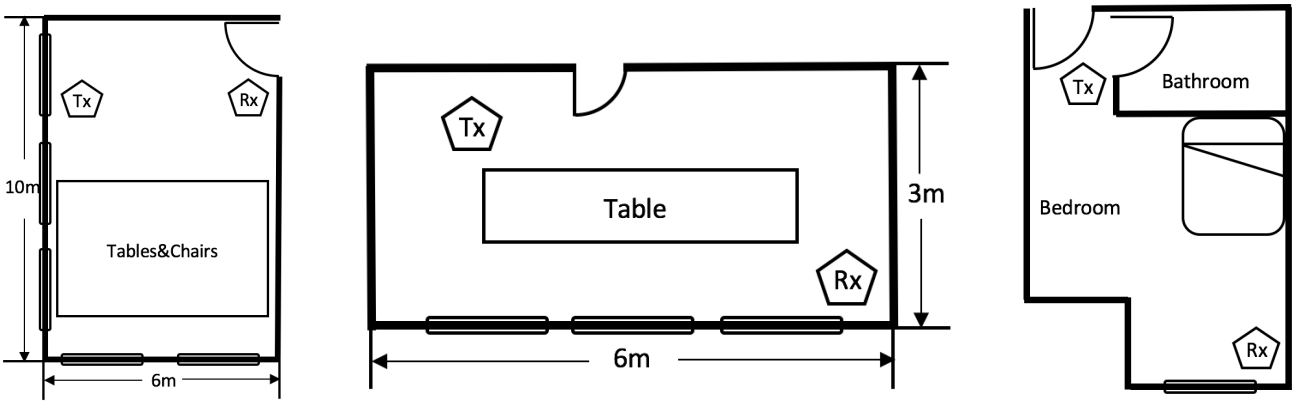

(a) Classroom. (b) Meeting Room (c) Dormitory Room

Figure 7. Floor plans.

and receiver. The node supports IEEE 802.11n standard and we choose one channel in 2.4 GHz ISM band to operate WiSH . The transmitting node is equipped with one antenna and the receiving node is equipped with three antennas. Thus there are three groups of CSI which correspond to three individual wireless links and we splice them together to create a whole matrix as Eqn. 3 shows. Different from traditional WiFi devices that are utilized to perform sensing applications (e.g, laptops and mini desktops), the node only uses 128MB DDR2 RAM. And limited by hardware capability, the highest sampling rate is around 15 $\sim$ 20Hz. It is much lower than the used sampling rate 100 $\sim$ 1000 Hz in prior work [2] [6] [13].

However, the node exhibits following favorable features. Firstly, it is in low energy levels. In standby mode (WiFi turned off), the power is merely 462 mW. The power increases to 660 mW when there is a small communication flow. And the power in full load mode is 990 mW. Secondly, the cost of the node is only 10 dollars. Furthermore, the node is portable and easy to be deployed. We use C language to implement the methodology and operate it in OpenWrt which is an embedded operating system based on Linux. In order to exhibit real-time detection results, we also build a website which can be depicted in Fig. 6. The red box indicates there are moving entities during this time duration.

To further investigate how sampling rate affect the performance of proposed methodology, we transfer the system to the traditional wireless platform. A TP-LINK TL-WDR7500 WiFi router that supports IEEE 802.11n standard works as the transmitter and a mini desktop (physical size 170 mm $\times$ 170 mm) with three antennas works as the receiver. The mini desktop is equipped with an Intel 5300 NIC and run Ubuntu 12.04 OS. With Linux 802.11n CSI Tool deployed, the mini-desktop is able to collect CSI measurements.

5 Evaluation

5.1 Experimental Settings

Our experiments can be classified into two categories. Firstly, to evaluate the performance of WiSH with tiny nodes deployed, we conduct experiments in a classroom, a meeting room and a dormitory room. The classroom is 6m $\times$ 10m large and the nodes are placed at the front of the classroom. In such case, we investigate how movement events at different locations, the distance between two nodes, the speed of the moving entity and other factors affect the performance of WiSH . And the effective covering range of WiSH can be determined via experiment results. The meeting room and dormitory room is 3m $\times$ 6m large and 3m $\times$ 4m large, respectively. WiSH is deployed in above scenarios to monitor whether there are intrusion or moving events. The two tiny nodes are placed along the diagonal of the room. The transmitting node is 4m away from the receiving node. Both are placed 1.2m high. The floor plans are depicted in Fig. 7.

Secondly, due to the limited hardware capacity of tiny nodes, we deploy the mini desktop and WiFi router in the classroom and meeting room to further investigate how sampling rate affects the performance of proposed methodology.

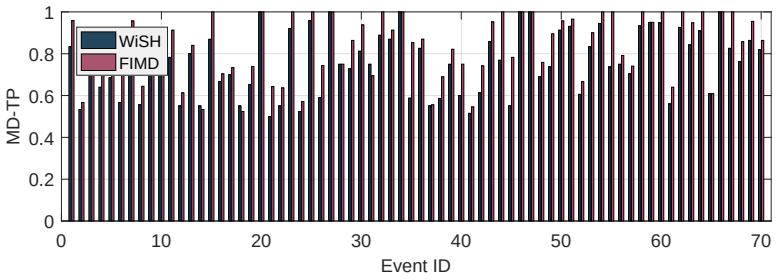

Figure 8. Detection Accuracy of WiSH and FIMD.

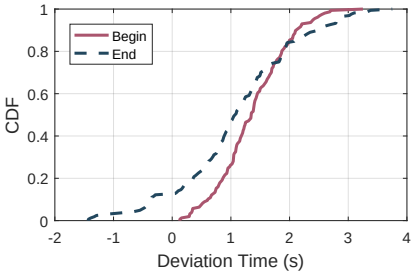

Figure 9. Distribution of event boundary error.

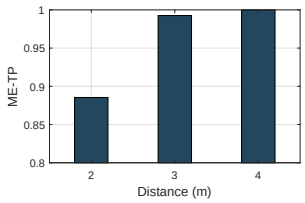

Figure 10. Impact of distance between transmitter and receiver.

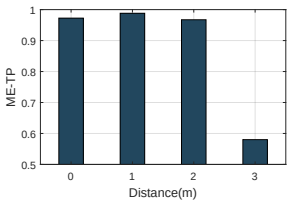

Figure 11. Impact of distance between human and LOS.

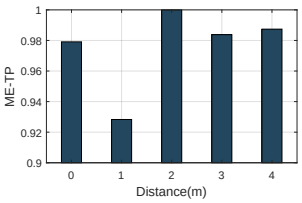

Figure 12. Impact of distance between human and transmitter.

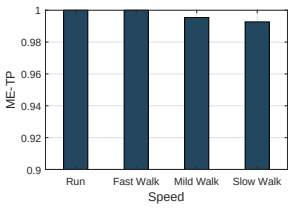

Figure 13. Impact of moving speed.

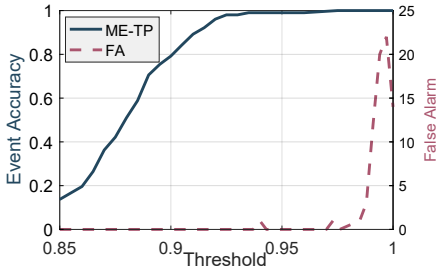

(a) Event detection and False alarm rate.

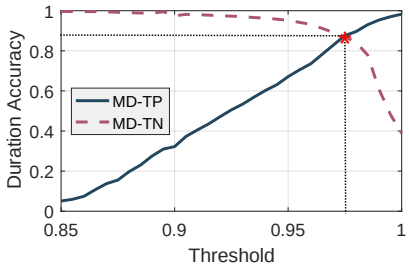

(b) ROC

Figure 14. Impact of threshold.

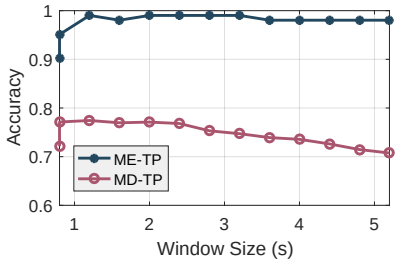

Figure 15. Impact of window size.

In order to obtain the ground truth of environment conditions, we place a 360 D600 camera which has a wide-angle lens around the receiver. The range of vision covers the monitoring area.

5.2 Performance

5.2.1 *Evaluation Metric*

We use following metrics to extensively evaluate the performance of our system and compare the performance with PADS [2] and FIMD [3].

- True Positive rate of Human Movement Event (ME-TP): ME-TP is the probability that a human presence event is correctly detected.
- False Alarm (FA): FA is the number of false alarms of movement events when there is actually no human presence.
- True Positive and True Negative rates of Human Movement Duration (denoted as MD-TP and MD-TN respectively): MD-TP (MD-TN) calculates the overlapping time periods between detected movement (non-movement) events and the ground truths.

Table 1
Overall Performance

Scenario	ME-TP	FA	MD-TP	MD-TN	MBE	MEE
Meeting room	98.83%	4	81%	91.45%	1.46s	2.95s
Dormitory room	98.58%	6	82%	94.25%	1.48s	2.08s

Table 2
Overall Performance among Different Sampling Number of Subcarriers

Sampling Number	ME-TP	FA	Deviation Time	Time Cost
90	98.75%	0	1.63s	2544.19s
45	98.75%	0	1.59s	740.36s
30	96.25%	0	1.67s	344.74s

- The Errors of Movement Beginning (MBE) and Ending Time (MEE): The delays (time biases with respect to ground truths) when an event is detected to start or end, respectively. Motion event's start means when user begins to move in the monitoring area and motion event's end means when user stops moving in the monitoring area.

5.2.2 Overall Performance

With tiny WiFi nodes deployed in the meeting room for one day and in the dormitory room for two days, we evaluate the overall performance of WiSH . The results are shown in Table 1.

We observe that ME-TP rate reaches over 98% in both scenarios. And MD-TP rate (duration accuracy) is relatively low compared with ME-TP rate (event accuracy). It is rational if we take the speed of the moving target, sensitiveness variety at different locations and other factors into consideration, which are comprehensively discussed hereinafter. False alarms can be further minimized if we choose a channel which suffers less radio frequency interference as there might exist other devices operate in the same channel.

To evaluate the real-time performance of the system, we calculate the deviation of boundaries of movement events. Table 1 shows the average MBE and MEE in the two scenarios. The time delay of detecting whether a movement event starts (MBE) cannot be avoided because we utilize a time series to perform human detection robustly as illustrated in Section 3.3. However, we believe the delays are tolerable considering the average time span of movement events. Note that MEE is much larger than MBE. The rationale lies in that CSI cannot be static as soon as the target stops moving. Thus MD-TN cannot reach 100% as well. Fig. 9 shows the distribution of MBE and MEE of 170 movement events that happened in the meeting room. It can be seen that median deviation is about 1.35s for the beginning time and 1.07s for the ending time. And 90 percent of motion events can be correctly detected with deviation less than 2.2s. Note that MEE can be a negative value because micro movements might be discarded by the system.

To prove the efficiency of our new method of picking before calculating cross correlation in frequency, this time we conduct on 17,005 records in tiny node. We choose different sampling number of subcarriers and in Table 2 we find that when sampling number is 45, it can guarantee ME-TP and desired deviation time, at the same time, the operation time is largely shortened.

We also operate FIMD [3] and PADS [2] on the tiny nodes to verify the lower computation complexity of WiSH and compare their detection accuracy. We choose the most representative evaluating indicator to evaluate these three methods. The difference among three systems is the methodology to calculate motion indicator (see Section 3.2). WiSH utilizes the correlation of CSI amplitude in both time domain and frequency domain. FIMD uses only time correlation of CSI amplitude and it adopts more sophisticated methods that calculate eigen-values of correlation matrix. PADS employs both amplitude and phase information to extract features and it also performs eigen-value decomposition. With CSI collected in 15 minutes as input, WiSH , FIMD and PADS use $0.0145s$, $0.8911s$ and $1.7765s$ respectively to calculate motion indicator. Thus PADS and FIMD cannot meet the requirement of real time if the system operates with a low sampling rate in the whole day. Fig. 8 shows the distribution of true positive rate of motion duration for 70 events. It can be seen that the performance of WiSH is comparable to that of FIMD, in terms of duration accuracy. However, WiSH avoids complex calculation of eigen-values and is more feasible for embedded devices which have limited computation resources.

5.2.3 Parameter Study

Now we study the impacts of different parameters on the system performance.

Impacts of Distance between Transmitter and Receiver. We conduct the experiments in a classroom. The distance between the transmitting node and receiving node varies from 2m to 4m. A volunteer is asked to walk evenly in a square area of 4m $\times$ 6m in which the nodes are placed. As Fig. 10 shows, when the distance decreases to 2m, ME-TP rate drops below 90%. The main reason is that if the nodes are placed too close, Line-of-Sight (LOS) will surpass other paths. Human movements exerts fewer impacts on CSI and WiSH fails to report some events. Thus we choose 4m as the proper distance between Tx and Rx for other parameter studies.

Impacts of Distance between Human and LOS. In order to determine the effective covering range of WiSH with tiny nodes deployed, a volunteer is asked to walk along a route which is parallel with LOS. The vertical distance between the route and LOS changes from 0m to 3m. We observe that with the distance increasing to 3m, ME-TP rate drops dramatically to around 58% as shown in Fig. 11. Thus if the moving target is located too far away from the nodes, it is probable that WiSH cannot work. We believe such problem, however, can be handled well if more nodes are deployed in the classroom.

Impacts of Distance between Human and Transmitter. If the moving event happens at different locations, CSI might suffer dynamics at different degrees. Therefore, we ask a volunteer to walk along a route which is perpendicular to LOS in order to validate the robustness of WiSH . The total length of the route is 6m. From Fig. 12, we find that ME-TP rate remains over 92% no matter how much the distance between human and transmitter exists. Thus we believe such factor exerts little influence on the performance of WiSH .

Impacts of Moving Speed. Fast human movements result in drastic changes of CSI amplitude in both time domain and frequency domain. However, the instantaneous velocity of slow movements is rather small and moving events cannot captured by simply employing the correlation property of CSI. Thanks to robust filter which is proposed in Section 3.3, WiSH is capable of detecting slow movements effectively as well. As Fig. 13 illustrates, WiSH remains high accuracy regardless of speed variations. Even if the moving target walks slowly in the monitoring area, ME-TP rate reaches over 99%.

Impacts of Detection Threshold. Intuitively, the larger detection threshold is, the more sensitive it performs. As shown in Fig. 14a, ME-TP increases with detection threshold increasing. However, when detection threshold exceeds 0.98, some correlation values in static cases are also below the threshold, and thus false alarm starts to increase. Fig. 14b shows the change of duration accuracy against detection threshold. Consistently, ME-TP increases and MD-TN decreases as detection threshold increases. While the balance point for duration accuracy is 0.975, we care more

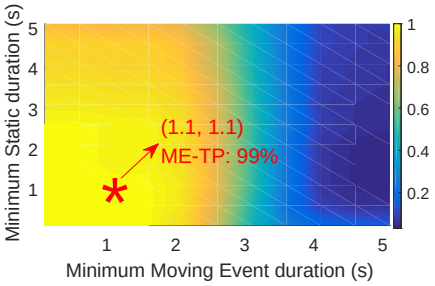

(a) Detection rate.

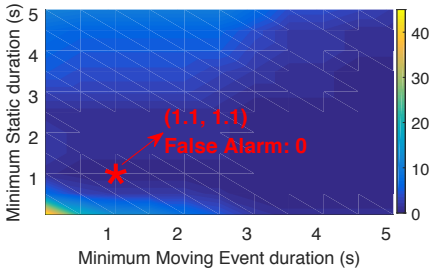

(b) False alarm.

Figure 16. Impact of minimum event length.

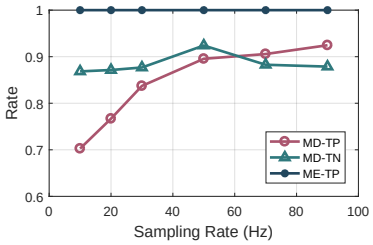

Figure 17. Impact of sampling rate.

about accurate ME-TP and fewer false alarms. Thus we choose 0.959 as final detection threshold.

Impacts of Sliding Window Size. Intuitively, the performance of WiSH will become better if the sliding window size is larger as the corresponding observation time is expanded. As shown in Fig. 15, ME-TP increases apparently when the window size increases to 2s. However, when the window size is too large, ME-TP will decrease instead. It is reasonable because when the duration of human movements is very small, the corresponding dynamic CSI measurements only occupy a small proportion compared with the static period. Thus the system will consider it as a static case and ME-TP falls.

Now we analyse how MD-TP is impacted by the sliding window size. When the window size gets smaller, the system will be more sensitive to human movements. Therefore, MD-TP increases as the window size decreases. Nevertheless, due to abrupt fluctuations of CSI which occasionally occur, overall performance will degrade when the window size is too small. Thus, we need to make a trade-off. And 1.2s can be regarded as a proper sliding window size.

Impacts of Thresholds in the Robust Event Filter As mentioned in Section 3.3, we need to adopt two thresholds d_1 and d_2 for fewer false alarms and human movements missing. We refer d_1 and d_2 to the minimum moving event duration and the minimum static event duration respectively. As shown in Fig. 16a, the value of d_1 exerts more influence on ME-TP than d_2 does. And false alarms decrease drastically with proper thresholds selected (see Fig. 16b). To ensure both high ME-TP rate and a small number of false alarms, we choose minimum moving event duration as 1.1s and minimum static event duration as 1.1s.

Impacts of Sampling Rate Although we aim to enable accurate movement detection with low sampling rate limitation (less than 20Hz) on our tiny nodes, we also evaluate and compare the performance under different sample rates. The experiments are conducted with the traditional wireless platform which consists of a router and a mini desktop. As Fig. 17 shows, MD-TN rate changes slightly with sampling rate increasing and ME-TP rate remains 100%. As increasing sampling rate results in more CSI measurements collected, the detection methodology will be more robust if the sliding window size does not vary. And we observe that the ratio of detected duration correctly overlapping with true events increases from 76.7% to 92.5% when the sampling rate increases from 20Hz to 90Hz.

6 Related Works

6.1 RF-based Passive Moving Human Detection

Considering that vision-based human detection systems [18]–[20] work with strict constraints (e.g., LOS and lighting) and require heavy computing, researchers have been devoted to finding alternatives. The concept of RF-based passive localization/detection originates in the work [21], [22] which aims to localize or track a person without carrying any RF devices. In order to implement device-free systems, many prior works utilize RSSI, which can be obtained from WiFi devices [23], ZigBee nodes [24], RFID readers [25], etc. The rationale lies in that the variance of RSSI becomes much larger when there are moving entities in the monitoring area. However, due to multipath effects and temporal dynamics, the performance of RSSI-based moving human detection algorithms might suffer dramatic degradation [26].

Then many research efforts have been devoted to CSI-based schemes as CSI can be exported from off-the-shelf NICs with slighter driver modification [16]. Compared with RSSI, CSI provides both amplitude and phase information. Besides, it is capable of discriminating multipath characteristics. Therefore, the performance can be largely improved by exploiting CSI. Based on the observation that the temporal correlation of CSI is much higher in static environment, [3] implements accurate fine-grained burst motion detection. Omni-PHD harnesses the histogram feature of the subcarrier amplitudes to implement omnidirectional passive human detection [15]. PADS [2] is the first effort to leverage phase information in passive target detection. R-TTWD [27] proposes a subcarrier dimension-based feature to implement through-the-wall detection. RoMD [28] also takes the impacts of antenna selection into consideration. Most prior works, however, still suffer from several limitations for real-time applications in practice. Typically, they usually require prior training, very high sample rate, and complex algorithms, which make them infeasible for energy-efficient and real-time applications. In this paper, we propose a lightweight system for real-time sensing of human detection. The system only requires very low sample rate and can work on embedded devices which have limited computation resources.

6.2 WiFi-based Activity Recognition

Apart from human presence detection, a large number of innovative applications and systems have emerged by exploiting WiFi, including localization [29]–[31], gesture recognition [5], [32], [33], gait recognition [6], smoking detection [7], sleep monitoring [9], [34], fall detection [10], respiration and heart rate monitoring [11], [35], etc. Recent works can be mainly divided into two categories. Some rely on location and environment-dependent features [4],e.g., CSI amplitude profiles. And the recognition model needs to be re-trained for each different scenario. Others extract environment-independent features from original CSI, such as velocity [36], [37] and Doppler shifts [32]. Many of work, however, still adopt learning-based solutions and rely on very rigorous requisites. Keystroke and activity recognition systems [4], [8], [13] use off-the-shelf WiFi devices and they require significant prior training at different locations in order to achieve high recognition accuracy. In order to achieve accurate localization and tracking in [12], [36], dense links are required to be deployed preliminarily. Sleep and respiration monitoring systems [9], [38] require users to be sufficiently close to the wireless links. Otherwise, the detection accuracy cannot be guaranteed. And most sensing applications only work in rather ideal environment without interference. In this paper, we design and implement a real-time passive human detection system that does not rely on the rigorous requisites and works in practice. WiSH employs lightweight but effective methods and enables detection even on resource-limited devices with rather low sampling rate.

7 Conclusions

In this paper, we present the design and implementation of WiSH , a real-time human presence detection system for whole-day usage. Considering various practical constraints, we propose a lightweight yet effective detection method based on both time and frequency correlations of CSI measurements. To sift out CSI eruptions due to irrelevant instantaneous motions or environmental changes, we further design a robust event filter to identify targeted human presence events. We implement WiSH on resource-limited RF devices and evaluate the performance in different scenarios. The results demonstrate that WiSH achieves remarkable detection accuracy of higher than 98%. With the sampling rate of 20Hz, the average detection delay is merely 1.5s and the durations of all detected events overlap with true events by 76.7%, which grows to 92.5% if the sampling rate increases to 90 Hz. We envision WiSH a practical system for real-time human detection in practice and will deploy WiSH at large scale for long-term monitoring in real world scenarios.

8 Future Work

In the detecting rectangle area, we can get result with high accuracy around the diagonal between sender and receiver tiny nodes. However, if human moves in the area far from this diagonal the system may not detect because of long distance and low sampling rate. To solve this problem, we can deploy more receiver nodes to cover detecting area as more as possible. Furthermore, We can combine data collected by all receiver nodes together to achieve higher accuracy, but how to synchronize is also a big challenge.

Also, in this paper, we only use CSI amplitude in both time domain and frequency domain and have already achieved high accuracy, but other parameters like noise-signal ratio have not been used yet. As we need to find a balance point between accuracy and operation time under limited computing environment, under the premise of short operation time we may try to use them to improve our model to get higher accuracy.

Acknowledgments

This work is supported in part by the NSFC under grant 61522110, 61332004 , 61472098, 61361166009, 61572366, 61602381, 61472057, National Key Research Plan under grant No. 2016YFC0700100.

References

[1] Z. Zhou, C. Wu, Z. Yang, and Y. Liu, "Sensorless Sensing with WiFi," *Tsinghua Science and Technology*, 2015.
[2] K. Qian, C. Wu, Z. Yang, Y. Liu, and Z. Zhou, "Pads: passive detection of moving targets with dynamic speed using phy layer information," in *Proceedings of IEEE ICPADS*, 2014.
[3] J. Xiao, K. Wu, Y. Yi, L. Wang, and L. M. Ni, "Fimd: Fine-grained device-free motion detection," in *Proceedings of IEEE ICPADS*, 2012.
[4] Y. Wang, J. Liu, Y. Chen, M. Gruteser, J. Yang, and H. Liu, "E-eyes: device-free location-oriented activity identification using fine-grained wifi signatures," in *Proceedings of ACM MobiCom*, 2014.
[5] Q. Pu, S. Gupta, S. Gollakota, and S. Patel, "Whole-home gesture recognition using wireless signals," in *Proceedings of ACM Mobicom*, 2013.
[6] W. Wang, A. X. Liu, and M. Shahzad, "Gait recognition using wifi signals," in *Proceedings of ACM Ubicomp*, 2016.
[7] X. Zheng, J. Wang, L. Shangguan, Z. Zhou, and Y. Liu, "Smokey: Ubiquitous smoking detection with commercial wifi infrastructures," in *Proceedings of IEEE INFOCOM*, 2016.
[8] M. Li, Y. Meng, J. Liu, H. Zhu, X. Liang, Y. Liu, and N. Ruan, "When csi meets public wifi: Inferring your mobile phone password via wifi signals," in *Proceedings of ACM SIGSAC CCS*, 2016.
[9] X. Liu, J. Cao, S. Tang, and J. Wen, "Wi-sleep: Contactless sleep monitoring via wifi signals," in *Proceedings of IEEE RTSS*, 2014.
[10] H. Wang, D. Zhang, Y. Wang, J. Ma, Y. Wang, and S. Li, "Rt-fall: A real-time and contactless fall detection system with commodity wifi devices," *IEEE Transactions on Mobile Computing*, 2016.
[11] J. Liu, Y. Wang, Y. Chen, J. Yang, X. Chen, and J. Cheng, "Tracking vital signs during sleep leveraging off-the-shelf wifi," in *Proceedings of ACM MobiHoc*, 2015.
[12] J. Wang, H. Jiang, J. Xiong, K. Jamieson, X. Chen, D. Fang, and B. Xie, "Lifs: Low human effort, device-free localization with fine-grained subcarrier information," in *Proceedings of ACM Mobicom*, 2016.
[13] B. Wei, W. Hu, M. Yang, and C. T. Chou, "Radio-based device-free activity recognition with radio frequency interference," in *Proceedings of ACM IPSN*, 2015.
[14] C. Wu, Z. Yang, Z. Zhou, X. Liu, Y. Liu, and J. Cao, "Non-invasive detection of moving and stationary human with wifi," *IEEE Journal on Selected Areas in Communications*, 2015.
[15] Z. Zhou, Z. Yang, C. Wu, L. Shangguan, and Y. Liu, "Towards omnidirectional passive human detection," in *Proceedings of IEEE INFOCOM*, 2013.
[16] D. Halperin, W. Hu, A. Sheth, and D. Wetherall, "Predictable 802.11 packet delivery from wireless channel measurements," in *Proceedings of ACM SIGCOMM*, 2011.
[17] Y. Xie, Z. Li, and M. Li, "Precise power delay profiling with commodity wifi," in *Proceedings of ACM MobiCom*, 2015.
[18] N. Dalal, B. Triggs, and C. Schmid, "Human detection using oriented histograms of flow and appearance," in *European conference on computer vision*, 2006.

[19] L. Xia, C.-C. Chen, and J. K. Aggarwal, "Human detection using depth information by kinect," in *Computer Vision and Pattern Recognition Workshops (CVPRW), 2011 IEEE Computer Society Conference on*, 2011.

[20] C. H. Morimoto, D. Koons, A. Amir, and M. Flickner, "Pupil detection and tracking using multiple light sources," *Image and vision computing*, 2000.

[21] M. Youssef, M. Mah, and A. Agrawala, "Challenges: device-free passive localization for wireless environments," in *Proceedings of ACM Mobicom*, 2007.

[22] L. Shangguan, Z. Yang, A. X. Liu, Z. Zhou, and Y. Liu, "Stpp: Spatial-temporal phase profiling-based method for relative rfid tag localization," in *IEEE/ACM Transactions on Networking (ToN)*, 2017.

[23] A. E. Kosba, A. Saeed, and M. Youssef, "Rasid: A robust wlan device-free passive motion detection system," in *Proceedings of IEEE PerCom*, 2012.

[24] D. Zhang, J. Ma, Q. Chen, and L. M. Ni, "An rf-based system for tracking transceiver-free objects," in *Proceedings of IEEE PerCom*, 2007.

[25] J. Han, C. Qian, X. Wang, D. Ma, J. Zhao, P. Zhang, W. Xi, and Z. Jiang, "Twins: Device-free object tracking using passive tags," in *Proceedings of IEEE INFOCOM*, 2014.

[26] Z. Yang, Z. Zhou, and Y. Liu, "From rssi to csi: Indoor localization via channel response," *ACM Comput. Surv.*, 2013.

[27] H. Zhu, F. Xiao, L. Sun, R. Wang, and P. Yang, "R-ttwd: Robust device-free through-the-wall detection of moving human with wifi," *IEEE Journal on Selected Areas in Communications*, 2017.

[28] G. Liu, Y. Li, D. Li, X. Ma, and F. Li, "Romd: Robust device-free motion detection using phy layer information," in *Proceedings of IEEE SECON*, 2015.

[29] C. Wu, Z. Yang, and Y. Liu, "Smartphones based crowdsourcing for indoor localization," in *IEEE Transactions on Mobile Computing (TMC)*, 2015.

[30] Z. Yang, C. Wu, Z. Zhou, X. Zhang, X. Wang, and Y. Liu, "Mobility increases localizability: A survey on wireless indoor localization using inertial sensors," in *ACM Computing Surveys*, 2015.

[31] C. Wu, Z. Yang, and C. Xiao, "Automatic radio map adaptation for indoor localization using smartphones," in *IEEE Transactions on Mobile Computing (TMC)*, 2018.

[32] K. Qian, C. Wu, Z. Zhou, Y. Zheng, Z. Yang, and Y. Liu, "Inferring motion direction using commodity wi-fi for interactive exergames," in *Proceedings of ACM CHI*, 2017.

[33] A. Virmani and M. Shahzad, "Position and orientation agnostic gesture recognition using wifi," in *Proceedings of ACM MobiSys*, 2017.

[34] C.-Y. Hsu, A. Ahuja, S. Yue, R. Hristov, Z. Kabelac, and D. Katabi, "Zero-effort in-home sleep and insomnia monitoring using radio signals," *Proceedings of ACM Ubicomp*, 2017.

[35] F. Adib, H. Mao, Z. Kabelac, D. Katabi, and R. C. Miller, "Smart homes that monitor breathing and heart rate," in *Proceedings of ACM CHI*, 2015.

[36] K. Qian, C. Wu, Z. Yang, Y. Liu, and K. Jamieson, "Widar: Decimeter-level passive tracking via velocity monitoring with commodity wi-fi," in *Proceedings of ACM MobiHoc*, 2017.

[37] W. Wang, A. X. Liu, M. Shahzad, K. Ling, and S. Lu, "Understanding and modeling of wifi signal based human activity recognition," in *Proceedings of ACM MobiCom*, 2015.

[38] H. Wang, D. Zhang, J. Ma, Y. Wang, Y. Wang, D. Wu, T. Gu, and B. Xie, "Human respiration detection with commodity wifi devices: do user location and body orientation matter?" in *Proceedings of ACM Ubicomp*, 2016.